LAWRENCE
LIVERMORE
NATIONAL
LABORATORY

Phase stability in heavy f-electron metals from first-principles theory

P. Soderlind

November 29, 2005

Disclaimer

Phase stability in heavy *f*-electron metals from first-principles theory

Per Söderlind
Physics and Advanced Technologies Directorate, Lawrence Livermore National Laboratory, Livermore, CA 94550, U.S.A.

ABSTRACT

The structural phase stability of heavy *f*-electron metals is studied by means of density-functional theory (DFT). These include temperature-induced transitions in plutonium metal as well as pressure-induced transitions in the trans-plutonium metals Am, Cm, Bk, and Cf. The early actinides (Th-Np) display phases that could be rather well understood from the competition of a crystal-symmetry breaking mechanism (Peierls distortion) of the 5*f* states and electrostatic forces, while for the trans-plutonium metals (Am-Cf) the ground-state structures are governed by 6*d* bonding. We show in this paper that new physics is needed to understand the phases of the actinides in the volume range of about 15-30 Å^3. At these volumes one would expect, from theoretical arguments made in the past, to encounter highly complex crystal phases due to a Peierls distortion. Here we argue that the symmetry reduction associated with spin polarization can make higher symmetry phases competitive. Taking this into account, DFT is shown to describe the well-known phase diagram of plutonium and also the recently discovered complex and intriguing high-pressure phase diagrams of Am and Cm. The theory is further applied to investigate the behaviors of Bk and Cf under compression.

INTRODUCTION

The understanding of the actinide metals is rapidly evolving due to recent progress in experimental and theoretical research. For some time now, it has been realized that many solid-state properties in these materials are determined by the bonding characteristics of the 5*f* orbitals, although a detailed understanding has been lacking. Certainly, the occurrence of complex crystal structures in the actinides, not present in other elements, seems to suggest that 5*f* bonding is the cause. The richness of phases and their detailed description as provided by experimental studies have proved to be an excellent testing ground for theory. In fact, DFT calculations were able to reproduce the structural behaviors of the light actinides and cerium very accurately [1].

The electronic-structure calculations of the actinides suggest that the low symmetry of especially the ground-state phases of uranium, neptunium, and plutonium is caused by the fact that 5*f* bands are pushed to unfavorably high and often degenerate energy levels when confined to high-symmetry configurations [2]. In the heavier actinides, Am and on, the 5*f*-band overlap is small at ambient conditions and poses a much smaller influence on the ground-state crystal structure which instead can be explained by 6*d* bonding in analogy to the rare-earth metals [3]. None of these two extreme situations of 5*f*-band involvement in the actinide bonding can be ascribed to the expanded phases of plutonium, or the moderately compressed phases of the trans-plutonium metals. Here we find a range of phases from high-symmetry face-centered cubic (fcc: δ-Pu, AmII, and CmII), lower symmetry face-centered orthorhombic (fco: γ-Pu, AmIII, and CmIV), and even lower symmetry primitive orthorhombic (po: AmIV and CmV). It appears

likely that the mechanisms stabilizing these phases are very similar and that one theoretical framework could either deal with all or none of them.

In the present work we have applied DFT that include spin and orbital effects to study this regime of the actinides and have focused on Pu [4], Am [5], Cm, Bk, and Cf.

COMPUTATIONAL DETAILS

The electronic structure and total energy are obtained from an all electron full-potential linear muffin-tin orbitals method. This implementation has been used extensively and successfully for transition and actinide metals [1,6] and allow for spin-orbit coupling, spin, and orbital polarization in the customary ways [7]. The "full potential" refers to the use of non-spherical contributions to the electron charge density and potential. This is accomplished by expanding these in cubic harmonics inside non-overlapping muffin-tin spheres and in a Fourier series in the interstitial region. We use two energy tails associated with each basis orbital and for the semi-core $6s$, $6p$, and valence $7s$, $7p$, $6d$, and $5f$ states, these pairs are different. Spherical harmonic expansions are carried out through $l_{max} = 6$ for the bases, potential, and charge density. For the electron exchange and correlation energy functional, the generalized gradient approximation is adopted [8].

The geometries of the crystal structures are kept fixed to the experimental geometry with the exception of some calculations for americium for which the structure is allowed to relax. Sampling of the irreducible Brillouin zone is done using the special k-point method [9] and the number of k points is large enough to converge the total energy to within 1 mRy/atom or less. In some cases this requires up to 2000 k points.

The calculations allows for spin polarization in ferromagnetic (FM) and antiferromagnetic (AF) configurations. The spin configurations of Pu and Am are generally AF, and they have been described in detail [4,5]. For the remaining Cm-Cf the total energies of the FM configuration is compared to the most naïve AF configurations. A complete search for the ground-state magnetic structure is not attempted. In some phases (Cf) the FM structure is predicted.

The equation of state for the respective phase is obtained from a fit of the total energies to a Murnaghan form [10]. Transition pressures are extracted from the total energies by a numerical fit, which is differentiated such that the Gibbs free energy is obtained. The transition is defined to occur when the free energy for the phases intersect. Finally, the calculations assume the Born-Oppenheimer assumption and are therefore relevant for low (zero) temperature.

PLUTONIUM

Plutonium may be the most exciting metal in the periodic table of elements. At atmospheric pressure it displays as many as six allotropes. Their atomic density and geometry varies in an extraordinary fashion and theoretically it is a most challenging scenario. Careful DFT can, however, predict total energies and atomic densities that are fully consistent with the experimental data, see Fig. 1. One unresolved issue is the theoretical prediction of the existence of substantial magnetic spin and orbital moments that has not been firmly confirmed by experiments. There are other theoretical approaches for δ-Pu that suppress this possibility, but none of these can accurately reproduce the equation of state for the other phases [4].
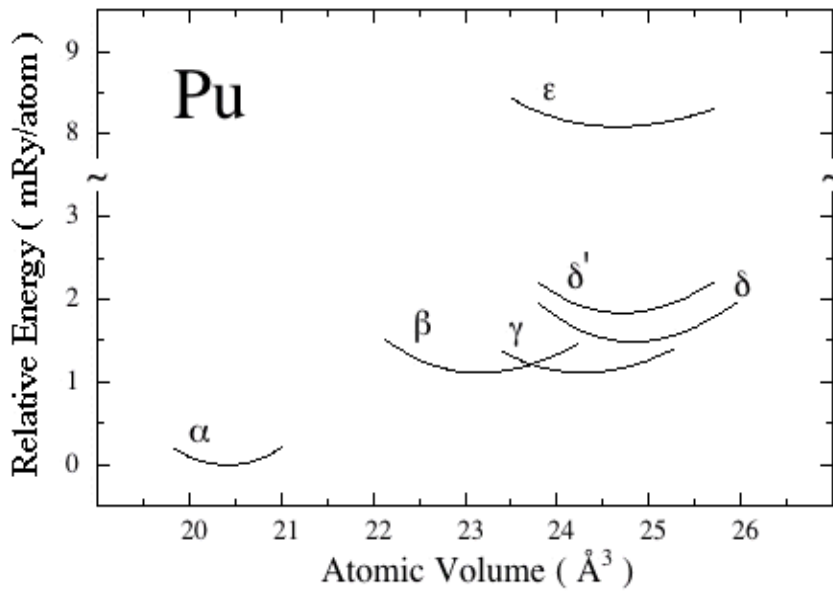
**Figure 1.** DFT total energies of the six known polymorphs of Pu.

$$F = E_{el} + E_{ph} - T(S_{ph} + S_{el})$$
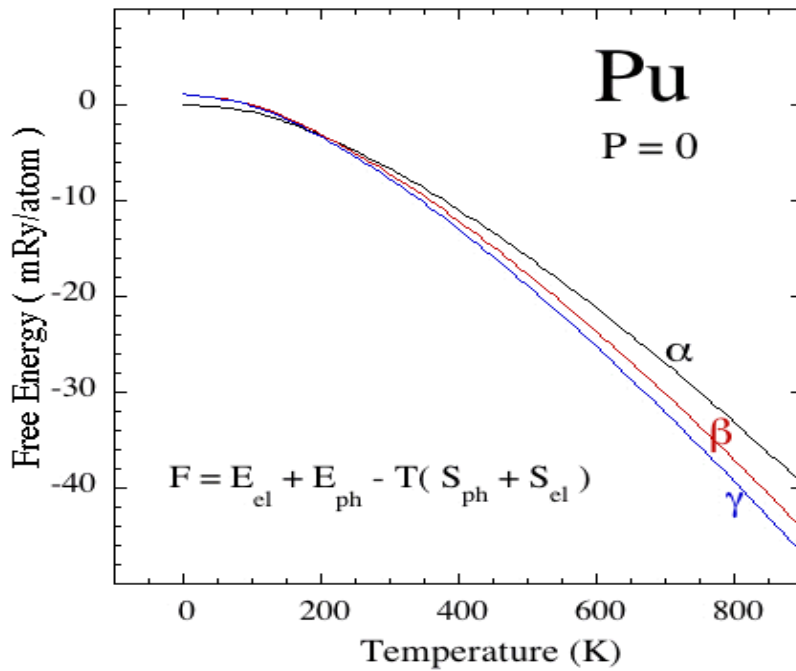
Figure 2. Helmholz free energies for Pu as obtained from DFT and Debye-Gruneisen theory.

From these total energies and the quasi-harmonic Debye-Gruneisen formalism [11], it is straight forward to construct the Helmholz free energy, Fig. 2. The free energies show that temperature indeed stabilizes both β and γ over the α phase in Pu.

AMERICIUM

There have been several experimental studies focused on the phase-behavior of americium under pressure (see Ref. 5 and references therein). They all agree that AmI and AmII are double-hexagonal close-packed (dhcp) and fcc, respectively, but the transition pressures as well as the structural assignments of the proceeding phases AmIII and AmIV have been controversial and confusing. For instance, AmIII was suggested to be monoclinic and AmIV of the α-U type. Later, theoretical calculations suggested that AmIV could not the α-U structure, but perhaps the α-Pu or the po α-Np structure [5]. Thankfully, americium was recently revisited experimentally [12] and AmIII and AmIV are now believed to be fco and po, respectively. DFT calculations later supported these new structural assignments [13].

There is little argument that the 5f electrons in Am are localized and chemically inert in its ground-state phase. Traditional DFT does not properly account for this localization as the preference for band formation dictate itinerant behavior of the 5f states. These itinerant states are indeed narrow and close to the Fermi level and the calculations predict spontaneous spin polarization. This obvious limitation of the theory turns out to be relatively unimportant because the almost complete spin polarization in Am represents a good approximation to the localized scenario. In Fig. 3 we show the total energies of dhcp (AmI) and fcc (AmII) phases that are nearly degenerate and within margin of error.
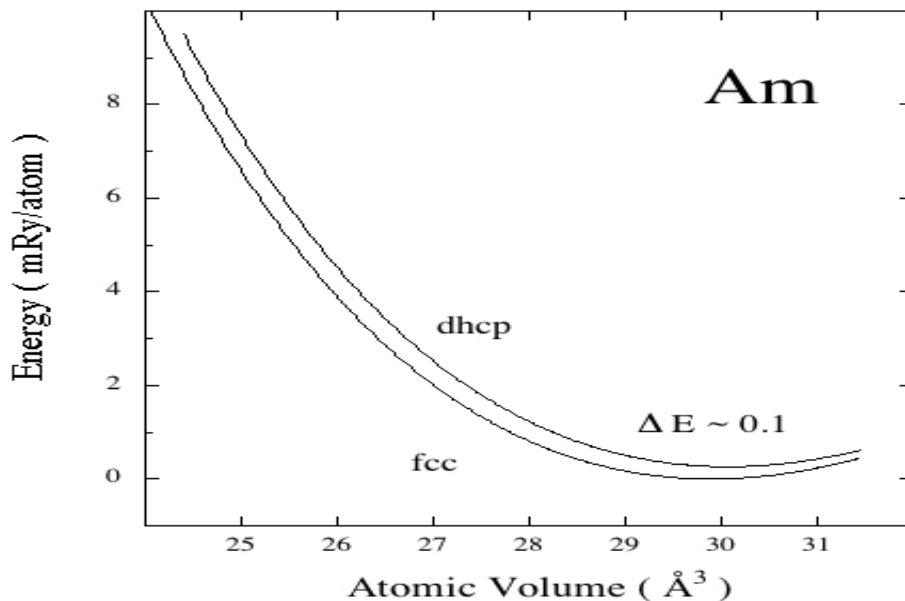
Figure 2. Practically indistinguishable total energies for fcc and dhcp Am.

In practice, the calculations predict the correct ground state with an equilibrium volume about 1% larger than the experimental volume. The theory is, however, unable to properly model the AmI –> AmII phase transition. Likely the presence of 5f electrons is somewhat overestimated.

At compressed volumes, Am is expected to have a greater degree of 5f-electron involvement in the atomic bonds (delocalization) and the deficiency of the theory, outlined above, is expected to diminish. Fig. 4 shows the total energies of AmII (fcc), AmIII (fco), AmIV (po) , and for comparison, the monoclinic α-Pu phase. The total energy of the α-U phase is much higher and not shown. From this data one obtains a transition from AmII –> AmIII at 107 kbar and AmIII –> AmIV at 158 kbar. This compares favorably with the latest known experimental transition pressures of 100 and 160 kbar, respectively [12]. It should be noted that the calculated transition pressures are sensitive to relaxation of especially the AmIII structure [5]. Furthermore, as pointed out [5], the new AmIV phase is close to the α-Np structure of the same po type, but less so to the often referred to α-U structure of the different fco type.
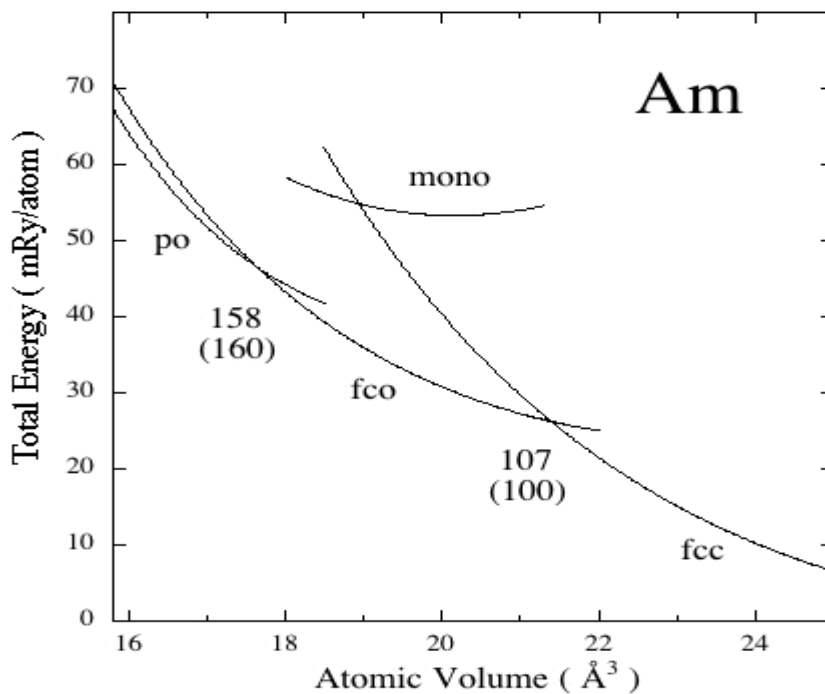
Figure 4. Total energies for fcc (AmII), fco (AmIII), po (AmIV), and monoclinic (α-Pu) Am.

Next, we show in Fig. 5 our theoretical equation of state together with recent experimental data [12]. Notice that our theory, with no adjustable parameters at all, follows the data very well throughout the entire pressure range. Recent DFT calculations for Am by Penicaud gave comparable results [13]. At compressions beyond this, canonical band theory [5] suggests the bcc phase to ultimately become stable. Calculated energy differences between the AmIV and bcc phases confirm this (not shown) [5].
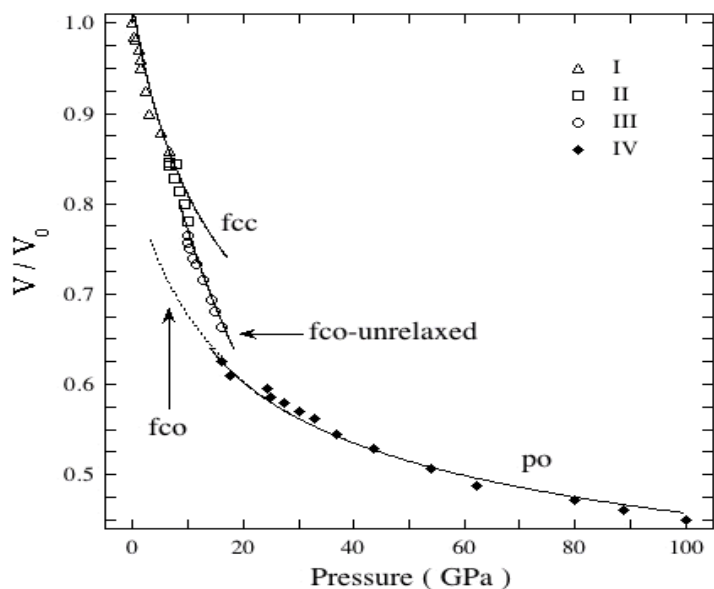
Figure 5. Theoretical (lines) and experimental equation of state for Am.
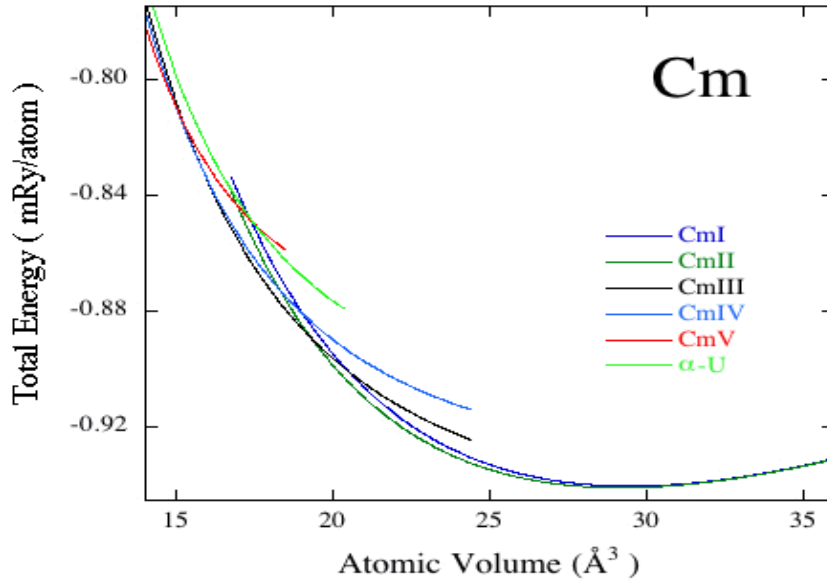
CURIUM

As in the case of Am, curium was recently revisited by synchrotron radiation determination of its high-pressure phases [14]. Although the initial dhcp and fcc phases (CmI and CmII) confirmed the previous assignments, new phases were found above about 400 kbar. The new CmIII is described as monoclinic with 2 atoms/cell. At about 560 kbar a transition to the new fco phase (also found in americium, AmIII, and plutonium, γ-Pu) was discovered. From this point on, curium behaves similar to Am with another phase transition to CmV (AmIV) at about 950 kbar. The two latter structures are well described in Refs. 5,12. Hence, as many as four pressure-induced phase transitions are determined experimentally for curium.

Theoretically, very few reports have been published for curium. Kutepov and Kutepova [15] predict an AF ground state, whereas Milman *et al.* [16] instead predicted a FM ground state. Our calculations agree with the former and in fact all phases in our study of curium are stable in the AF configuration.

In Fig. 6 we show total energies for CmI-CmV, and the α-U type structure for comparison. Notice that the CmII (fcc) structure is slightly stable over the CmI (dhcp) at ambient pressure, although the phases have nearly degenerate total energies. This is a deficiency of our theoretical approach to model a state with localized $5f$ electrons, as was also the case in Am. The calculations confirm the possibility of the phase transitions CmII –> CmIII, CmIII –> CmIV, and CmIV –> CmV, and exclude the α-U type structure. This is in good agreement with the

measurements and theoretical calculations presented in Ref. 14. In Fig. 7 we compare the

Figure 6. Total energies for CmI-CmV and α-U type structure for curium.
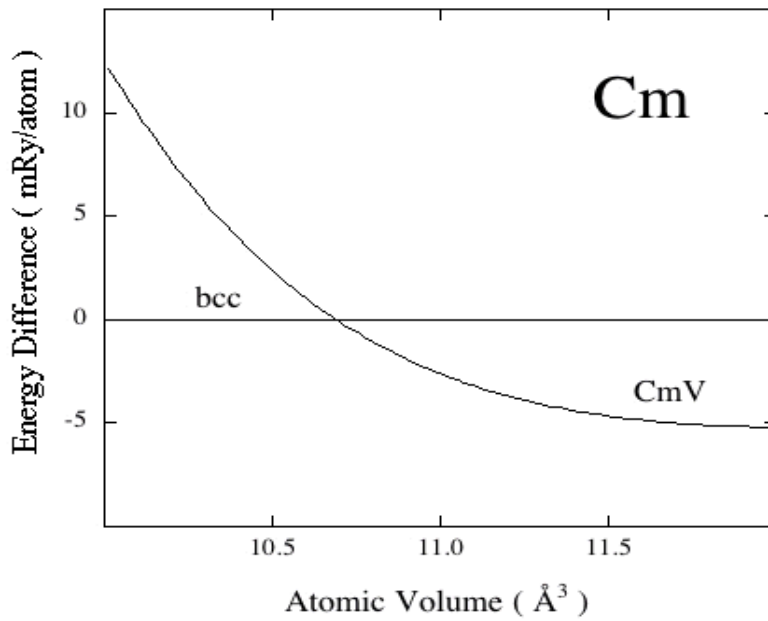
**Figure 7.** Total energy difference between CmV and bcc curium.

energies of CmV and bcc, and similar to Am and many other actinides, Cm stabilizes in the bcc phase at sufficiently high compression.

One of the main points of Ref. 14 was that CmIII (and presumable the other phases) are stabilized by itinerant magnetism. We agree with this conjecture and in Fig. 8 we present the total energies for CmIII-CmV in their AF and non-magnetic states. Clearly, the calculations predict a spontaneous magnetization as the AF energies are much lower than the non-magnetic ones. Notice also that at larger volumes the non-magnetic and AF calculations show the phases to order opposite, whereas at smaller volumes the order of the phases in the AF treatment is reversed and agree with those of the non-magnetic approximation. Hence, the CmIII –> CmIV and CmIV –> CmV phase transitions are a direct consequence of the effects of spin polarization. Fig. 8 also suggests that the non-magnetic assumption is a better approximation at higher compressions.
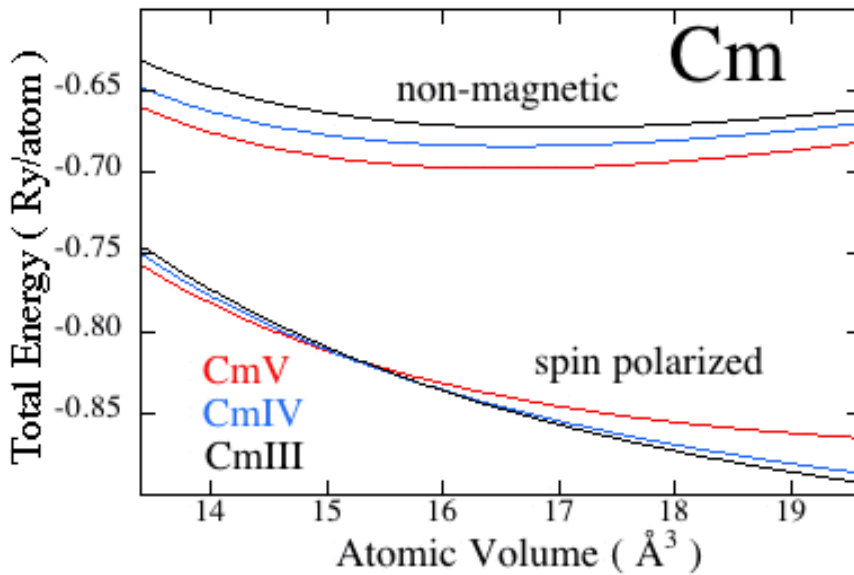
Figure 8. Total energies for AF and non-magnetic phases of Cm.

Finally for curium, we compare calculated equation of state with experimental data graciously provided by the authors of Ref. 14. The theory is represented with full lines and the phases are indicated as dhcp (CmI), mono (CmIII), fco (CmIV), and po (CmV). Because theoretical dhcp and fcc Cm equation of states are practically identical the fcc phase is omitted. The experimental phase transitions are marked with vertical lines. As mentioned, the CmI –> CmII transition cannot be reproduced by theory, but the calculated transition pressure for stabilization of the CmIII phase is 280 kbar with a 6% volume collapse from the close-packed phase. Experimentally this transition occurs closer to 380 kbar with a smaller volume collapse of about 4.5%. Theoretically, the CmIV phase is stabilized at about 480 kbar and remains stable to about 560 kbar. It is found to be stable by the measurements at higher pressures, from about 560 up to almost 1 Mbar, where CmV shows up. The calculations do confirm also the CmV phase but already at considerably lower pressure.
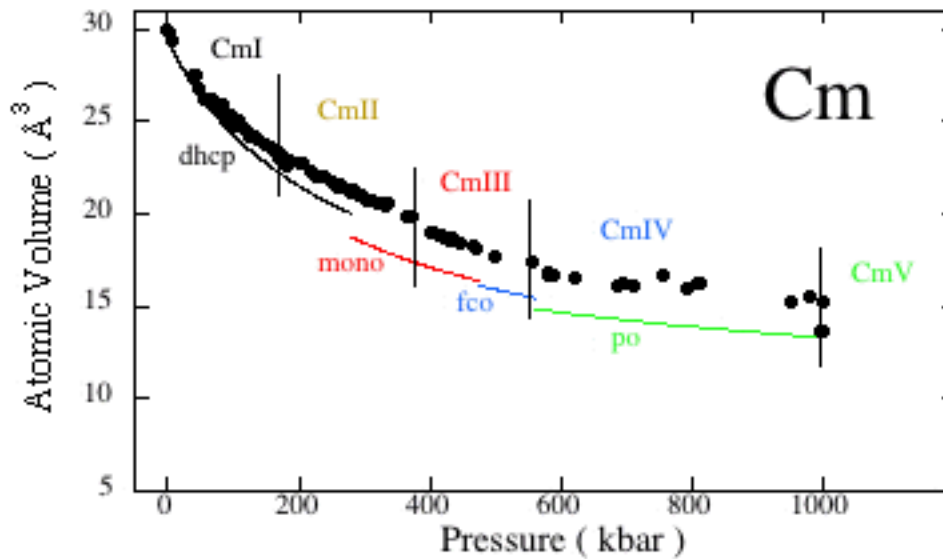
Figure 9. Theoretical and experimental equation of state for Cm.

The overall agreement between theory and experiment is not as good as for Am. Theory tends to predict larger volume collapses for the intermediate phases. It is remarkable, however, that all three CmIII-CmV phases are accounted for by theory. Hopefully experimental work is motivated by the theoretical prediction of a bcc phase at high compression.

BERKELIUM AND CALIFORNIUM

For Bk or Cf there are no recent experimental data available in contrast to Am and Cf. There were high-pressure studies of these heavy actinides a couple of decades ago [17]. They proposed a high-pressure α-U type structure at the onset of a $5f$ delocalization, similar to what the believed behavior was for Am and Cm at the time. The new revelations for both Am and Cm cast doubt on the earlier proposed high-pressure phases in Bk and Cf. There are no a priori reasons to believe that their high-pressure behavior should be substantially different from that of Am and Cm. Hence, we have performed total energy calculations for the same phases we have been dealing with so far, namely close-packed, CmIII-CmV, bcc, and the α-U type structure.

The Bk energy differences between these structures (except dhcp), relative to the bcc phase, are plotted in Fig. 10. Two phase transitions are proposed by the calculations. First, fcc –> CmIV at about 190 kbar and second, CmIV –> bcc, at about 740 kbar. The theory clearly rules out the α-U type structure, whereas the CmV, for instance, is not far from being stable and can thus not be firmly discarded. Also the CmIV and the bcc total energies are very close which makes the
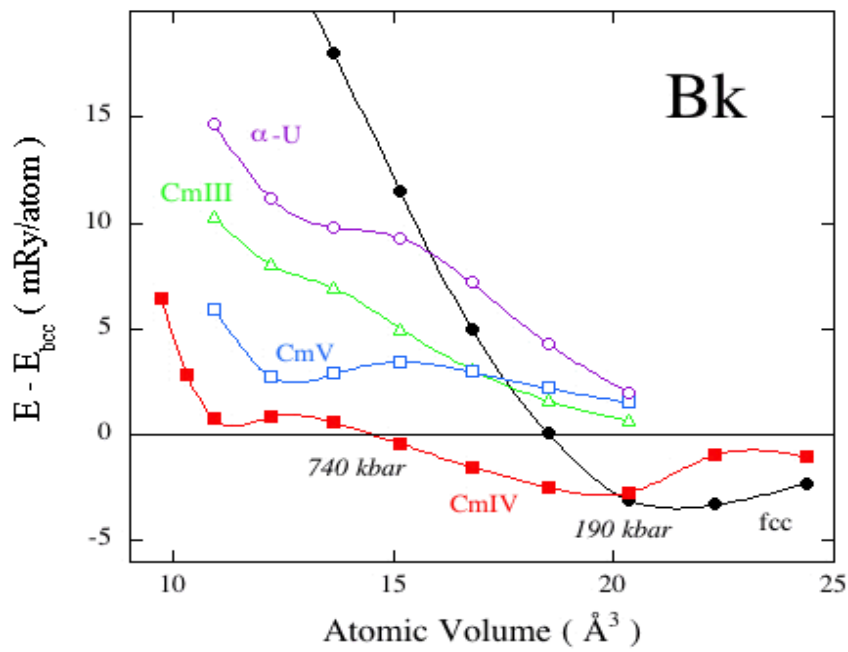
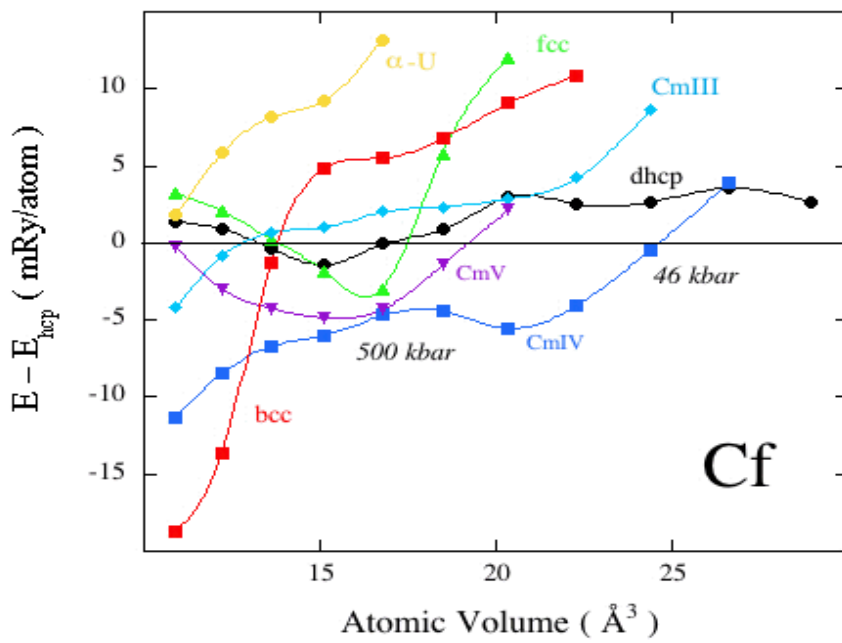**Figure 10.** Total energy differences for various phases of Bk.

Figure 11. Total energy differences for various phases of Cf.

calculated transition pressure to the bcc phase rather uncertain. From about 12 Å^3 all phases becomes increasingly unstable relative to the bcc phase, however.

Next, we show a similar graph for Cf in Fig. 11, now with all energies relative to the hcp structure. Again, the CmIV phase is very competitive and a possible candidate in the Cf phase diagram. At a modest pressure of only 46 kbar the calculations predict a phase transition to CmIV from the close-packed (hcp) phase. At about 500 kbar there are at least two other phases close in energy to the CmIV phase, which may indicate that yet another phase in reality might be stable. Again, as for Am-Bk, theory dictates a bcc phase at higher compressions.

It is noteworthy to mention that although the AF configurations are preferred theoretically for the trans-plutonium metals, this is not necessarily the case for all phases of Cf. Most phases go through a magnetic transition from AF to FM during compression. In Fig. 12 we show this for the dhcp phase. It is unclear why Cf, and not Am-Bk, displays this interesting behavior.
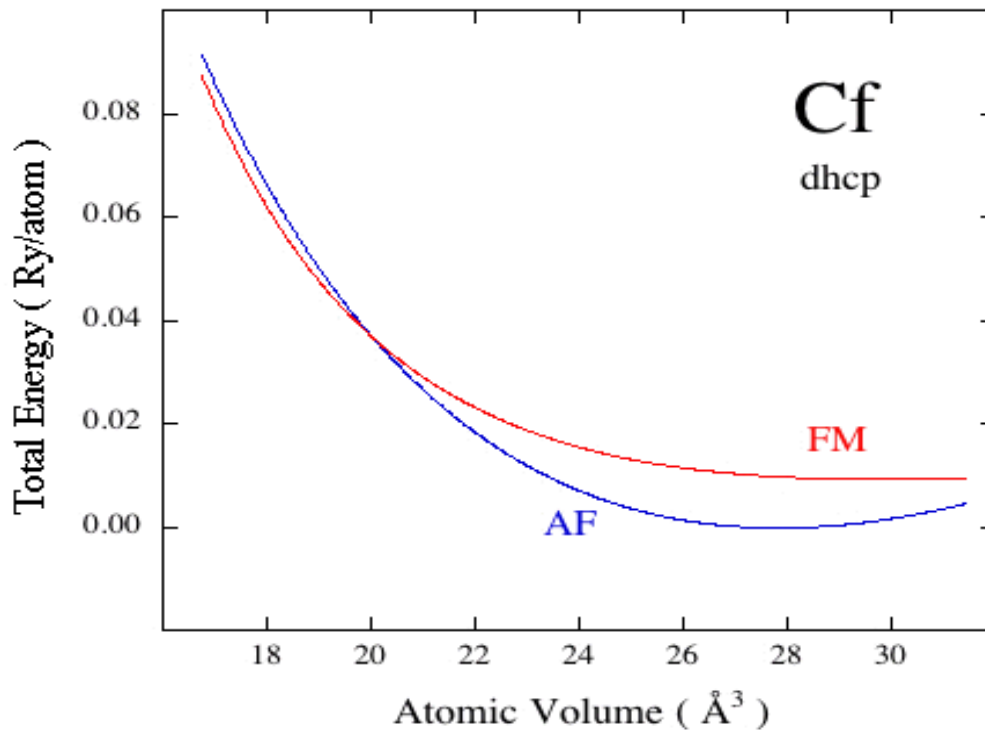
Figure 12. Magnetic phase transition in dhcp Cf.

We are now able to compare the sensitivity to delocalization in the heavy actinides. Our calculated transitions from close-packed to lower symmetry phases are 107, 280, 190, and 46 for Am-Cf. I.e., Cm (280) requires greater pressure for delocalization than its neighbors Am (107) and Bk (190). This trend is observed also in experiments [17] and the reason is likely that Cm has a 5f^7 half-filled shell which maximizes the energy gain associated with localization. This

particularly stable situation is more resistant to pressure than its neighbors Am and Bk as previously discussed [17].

ACKNOWLEDGMENTS

REFERENCES

1. P. Söderlind, Adv. Phys. **47**, 959 (1998).
2. P. Söderlind, O. Eriksson, B. Johansson, and J.M. Wills, and A.M. Boring, Nature (London) **374**, 524 (1995).
3. H.L. Skriver, Phys. Rev. B **31**, 1909 (1985); J.C. Duthie and D.G. Pettifor, Phys. Rev. Lett. **38**, 564 (1977).
4. P. Söderlind and B. Sadigh, Phys. Rev. Lett. **92**, 185702 (2004).
5. P. Söderlind and A. Landa, Phys. Rev. B **72**, 024109 (2005); P. Söderlind *et al., ibid.* **61**, 8119 (2000).
6. R. Ahuja, P. Söderlind, J. Trygg, J. Melsen, J.M. Wills, B. Johansson, and O. Eriksson, Phys. Rev. B **61**, 8119 (2000).
7. O.K. Andersen, Phys. Rev. B **12**, 3060 (1975); O. Eriksson, M.S.S. Brooks, and B. Johansson, Phys. Rev. B **41**, 9087 (1990); P. Söderlind, Europhys. Lett. **55**, 525 (2001).
8. J.P. Perdew, J.A. Chevary, S.H. Vosko, K.A. Jackson, M.R. Pederson, D.J. Singh, Phys. Rev. B **46**, 6671 (1992).
9. D.J. Chadi and M.L. Cohen, Phys. Rev. B **8**, 5747 (1973); S. Froyen, *ibid.* **39**, 3168 (1989).
10. F.D. Murnaghan, Proc. Natl. Acad. Sci. U.S.A. **30**, 244 (1944).
11. P. Söderlind, L. Nordström, L. Yongming, and B. Johansson, Phys. Rev. B 42, 4544 (1990).
12. S. Heathman *et al.*, Phys. Rev. Lett. **85**, 2961 (2000); A. Lindbaum *et al.*, Phys. Rev. **B** 63, 214101 (2001).
13. M. Penicaud, J. Phys.: Condens. Matter **17**, 257 (2005).
14. S. Heathman, R.G. Haire, T. Le Bihan, A. Lindbaum, M. Idiri, P. Normile, S. Li, R. Ahuja, B. Johansson, and G.H. Lander, Science **309**, 110 (2005).
15. A.L. Kutepov and S.G. Kutepova, J. Magn. Magn. Mat. **272-276**, e329 (2004).
16. V. Milman, N. Winkler, and C.J. Pickard, J. Nucl. Mat. **322**, 165 (2003).
17. U. Benedict *et al.*, J. Phys. F: Met. Phys. **14**, L43 (1984); J.P. Itie *et al., ibid.* **15**, L213 (1985).